

# Models for Multiscale Interactions I: A multcloud model parameterization

BOUALEM KHOUIDER \*

*Department of mathematics and statistics, University of Victoria, Victoria, British Columbia, Canada*

ANDREW J. MAJDA

*Center for Atmosphere-Ocean Science and Department of Mathematics, Courant Institute, New York University, New York, NY.*

---

\* *Corresponding author address:* Dr. Boualem Khouider, Mathematics and Statistics University of Victoria  
PO BOX 3045 STN CSC Victoria, B.C. Canada V8W 3P4.

Email: [khouider@math.uvic.ca](mailto:khouider@math.uvic.ca)

## ABSTRACT

In this chapter, we present a model parameterization for organized tropical convection and convectively coupled tropical waves. The model is based on the main three cloud types: congestus, deep, and stratiform that are observed to play an important role in the dynamics and morphology of tropical convective systems. The model is based on the self-similarity across scales of tropical convective systems and uses physically sound theory about the mutual interactions between the three cloud types and the environment. Both linear analysis and numerical simulations of convectively coupled waves and the Madden-Julian oscillation are discussed.

## 1. Introduction

Convection in the tropics is organized on hierarchy of scales ranging from the convective cell of a few kilometers to planetary scale disturbances such as the Madden-Julian oscillation (MJO). Cloud clusters and superclusters occur on the meso- and synoptic scales and often appear imbedded in each other and within the MJO envelope. Analysis of outgoing longwave radiation cross-correlated with the reanalysis products helped identify the synoptic scale superclusters as the moist analogs of the equatorial shallow water waves of Matsuno (1966) but with a severally reduced phase speed (Takayabu 1994; Wheeler and Kiladis 1999) and a front-to-rear vertical tilt in zonal wind, temperature, heating, and humidity profiles (Wheeler et al. 2000; Straub and Kiladis 2002). These moisture-coupled waves are often referred to as convectively coupled waves (Takayabu 1994; Wheeler and Kiladis 1999; Wheeler et al. 2000; Kiladis et al. 2009, CCWs). Convectively coupled Kelvin waves associated with the deepest

baroclinic mode dominate the spectral variability on the synoptic scales and propagate, along the equator, at speeds ranging from 12 to 20 m s<sup>-1</sup>, unlike their dry counterpart that travels at 50 m s<sup>-1</sup> (Kiladis et al. 2009).

For almost a decade, simple primitive equation models involving a single baroclinic vertical mode, forced by deep convection, have been used with some relative success for theoretical and numerical studies of various strategies for convectively coupled waves (Emanuel 1987; Mapes 1993; Neelin and Yu 1994; Yano et al. 1995, 1998; Majda and Shefter 2001b; Fuchs and Raymond 2002; Majda and Khouider 2002); They were somewhat able to reproduce scale selective instability, at the synoptic scale, of Kelvin waves with a propagation speed in the observed range. However, these one-baroclinic mode model fail to reproduce the important<sup>1</sup> front-to-rear tilt in the vertical and many other important features of CCWs. Moreover, these early models are based on two major theories for the destabilization of large-scale waves by convection, namely convergence-driven models and quasi-equilibrium models. Convergence models date back to the work of Charney and Eliassen (1964) followed by Yamasaki (1969); Hayashi (1971); Lindzen (1974). The convergence models, also called convective instability of second kind (CISK) models, sustain convection through large reservoirs of convectively available potential energy (CAPE) driven by low-level convergence. Such models exhibit extreme sensitivity to grid scale behavior and linearized stability analysis reveals the undesirable feature of catastrophic instability with growth rates increasing with wavenumber (Yano et al. 1998; Majda and Shefter 2001b). In the quasi-equilibrium thinking, first introduced by Arakawa and Shubert (1974), ones assumes a large scale quasi-equilibrium state where CAPE

---

<sup>1</sup>As we will see in Chap. 15, the vertical tilt is important for momentum transport from convective systems towards larger scales

is nearly constant and deep convection acts as an energy regulator in restoring quickly the equilibrium by consuming any excess of CAPE. The triggering and the amplification of convection in quasi-equilibrium models relies on surface fluxes. Indeed, such quasi-equilibrium models are linearly (Neelin and Yu 1994) and even nonlinearly stable (Frierson et al. 2004). The most popular mechanism used in concert with the quasi-equilibrium models to create instability is wind induced surface heat exchange (WISHE) (Emanuel 1987; Emanuel et al. 1994). Both WISHE and CISK theories were initially proposed for hurricanes (Zehnder 2001; Craig and Gray 1996). There is no basic observational evidence for their validity for CCWs (Straub and Kiladis 2003). The phenomenon of phase-speed reduction is associated, in these one-baroclinic mode models, solely to a reduction in the background stratification due to moisture coupling of the waves but the observed backward vertical tilt is a suggestive of a strong projection of the CCWs on shallower vertical modes, that have much slower gravity-wave speeds, in addition to the prominence of the fastest first baroclinic mode.

Recent analysis of observations over the warm pool in the tropics reveals the ubiquity of three cloud types above the boundary layer: shallow congestus clouds, stratiform clouds, and deep penetrative cumulus clouds (Lin and Johnson 1996; Johnson et al. 1999). Furthermore, recent analysis of convectively coupled waves on the large scales reveals a similar multi-cloud convective structure with leading shallow congestus cloud decks which moisten and precondition the lower troposphere followed by deep convection and finally trailing decks of stratiform precipitation; this structure applies to the eastward propagating convectively coupled Kelvin waves (Wheeler and Kiladis 1999; Straub and Kiladis 2002) and westward propagating two-day waves (Haertl and Kiladis 2004) which reside on equatorial synoptic scales of order 1,000 to 3,000 km in the lower troposphere as well as the planetary scale

Madden-Julian oscillation (Kiladis et al. 2005; Dunkerton and Crum 1995). An inherently multi-scale theory for the Madden-Julian oscillation with qualitative agreement with observations which is based on these three cloud types is proposed by Majda and Biello (2004); Biello and Majda (2005).

Furthermore, despite the observational evidence, none of the models with a single vertical mode mentioned earlier account for the multi-mode nature of tropical convection and the importance of the different cloud types; They are forced by a heating profile based solely on the deep-penetrative clouds. Parametrizations with two convective heating modes systematically representing, a deep-convective mode and a stratiform mode, have first appeared in the work of Mapes (2000). Majda and Shefter (2001a) proposed and analysed a simpler version of Mapes' model based on a systematic Galerkin projection of the primitive equations onto the first two linear-baroclinic modes yielding a set of two shallow water systems. The first baroclinic system is heated by deep convective clouds while the second baroclinic system is heated aloft and cooled below by stratiform anvils. Linear stability analysis of this model convective parametrization revealed a mechanism of stratiform instability independent of WISHE (Majda and Shefter 2001a; Majda et al. 2004). Numerical simulations carried out in (Majda et al. 2004) revealed the resemblance of many features of the moist gravity waves for the Majda and Shefter (2001a) model and the real world convective superclusters (Straub and Kiladis 2002; Majda et al. 2004). One visible shortcoming of the Majda and Shefter model is however its short-cutting of the role of the congestus heating and the systematic interaction of the cloud types with moisture.

## 2. The multcloud model

In a seminal paper, the authors (Khouider and Majda 2006b), proposed a new model convective parametrization, within the framework of the MS model. In addition to the deep convective and stratiform clouds, the new model carries cumulus congestus clouds which serve to heat the second baroclinic mode from below and cool it from above as in actual congestus cloud decks.

To help the visualization, a cartoon of the cloud types is shown in Figure 1 together with the associated heating profiles. The first baroclinic mode is heated by deep convection, as in the simple one-baroclinic-mode models discussed above, and the second baroclinic mode is heated and cooled by both congestus and stratiform clouds. Congestus clouds lead tropical convective systems and precondition the environment prior to deep convection. They heat the lower troposphere through condensation and induce a cooling of the upper troposphere through longwave radiation. Stratiform clouds, on the other hand, are observed to trail behind deep convection, and they heat the upper troposphere as deep clouds enter their freezing phase and cool the lower troposphere due to the evaporation of stratiform rain that falls into the already dry environment.

The minimal dynamical core for the multcloud model consists of two coupled (linear) shallow systems: forced and coupled through the heating rates associated with the three cloud types:

$$\begin{aligned}
 \frac{\partial \mathbf{v}_j}{\partial t} + \beta y \mathbf{v}_j^\perp - \nabla \theta_j &= -C_d(u_0) \mathbf{v}_j - \frac{1}{\tau_W} \mathbf{v}_j, \quad j = 1, 2, \\
 \frac{\partial \theta_1}{\partial t} - \text{div } \mathbf{v}_1 &= \frac{\pi}{2\sqrt{2}} P + S_1 \\
 \frac{\partial \theta_2}{\partial t} - \frac{1}{4} \text{div } \mathbf{v}_2 &= \frac{\pi}{2\sqrt{2}} (-H_s + H_c) + S_2,
 \end{aligned} \tag{1}$$

where the two modes  $j = 1$  and  $2$  are coupled through the nonlinear source terms. These equations are derived through a systematic Galerkin projection of the equatorial beta-plane primitive equations onto the first and second baroclinic modes that are directly forced by the heating rates,  $H_c, H_d, H_s$ , associated with the three cloud types. The nonlinear advection terms are neglected for simplicity; they are believed to play a secondary role in the presence of convective heating. The other source terms represent radiative cooling rates:  $S_j = -Q_{R,j}^0 - \frac{1}{\tau_R}\theta_j, j = 1, 2$ . Following Khouider and Majda (2008b), the total precipitation is set to  $P = H_d + \xi_s H_s + \xi_c H_c$ , and it includes contributions from deep convection, stratiform, and congestus clouds. Here  $\xi_s$  and  $\xi_c$  are parameters, between 0 and 1, representing the relative contributions of stratiform and congestus clouds to surface precipitation.

In addition to this dynamical core (1), there are equations for the boundary layer equivalent potential temperature,  $\theta_{eb}$ , and the vertically integrated moisture content,  $q$ :

$$\begin{aligned} \frac{\partial \theta_{eb}}{\partial t} &= \frac{1}{h_b}(E - D) \\ \frac{\partial q}{\partial t} + \text{div}((\mathbf{v}_1 + \tilde{\alpha}\mathbf{v}_2)q) + \tilde{Q} \text{div}(\mathbf{v}_1 + \tilde{\lambda}\mathbf{v}_2) &= -P + \frac{1}{H_T}D \end{aligned} \quad (2)$$

Here,  $h_b \approx 500$  meters is the height of the moist boundary layer while  $\tilde{Q}, \tilde{\lambda}$ , and  $\tilde{\alpha}$  are parameters associated with a prescribed moisture background and perturbation vertical profiles. According to the first equation in (2),  $\theta_{eb}$  changes in response to the downdrafts,  $D$ , and the sea surface evaporation  $E$ . When setting closure for the forcing terms in (2), conservation of vertically integrated moist-static energy is used as design principle. The moisture equation in (2) is derived through a systematic vertical averaging of the water vapor conservation equation (Khouider and Majda 2006b,a). The parameter  $\tilde{\lambda}$  measures the strength of moisture convergence due to the second baroclinic mode, and it plays an important role in the

dynamics of convectively coupled tropical waves (Khouider and Majda 2006b).

The main nonlinearities of the model are in the source terms  $H_d, H_c, H_s$ , and  $D$ . The stratiform and congestus heating rates,  $H_s$  and  $H_c$ , satisfy relaxation-type equations:

$$\frac{\partial H_s}{\partial t} = \frac{1}{\tau_s} (\alpha_s H_d - H_s) \quad (3)$$

and

$$\frac{\partial H_c}{\partial t} = \frac{1}{\tau_c} \left( \alpha_c \frac{\Lambda - \Lambda^*}{1 - \Lambda^*} Q_c - H_c \right). \quad (4)$$

The deep convective heating,  $H_d$ , and the downdrafts,  $D$ , are given diagnostically by

$$H_d = \frac{1 - \Lambda}{1 - \Lambda^*} Q_d \quad \text{and} \quad D = \Lambda D_0. \quad (5)$$

The “moisture switch” function  $\Lambda$  controls the transition between congestus to deep convection, and it depends on the difference between boundary layer and midtropospheric equivalent potential temperatures,  $\theta_{eb} - \theta_{em}$ . The diagnostic functions  $Q_d, Q_c, D_0$ , and  $\Lambda$  all involve nonlinear switches, and they are described in detail in Khouider and Majda (2008b). As an example,  $Q_d$  takes the form

$$Q_d = \left[ \bar{Q} + \frac{1}{\tau_{conv}} (a_1 \theta'_{eb} + a_2 q' - a_0 (\theta'_1 + \gamma_2 \theta'_2)) \right]^+. \quad (6)$$

Here and elsewhere in the paper,  $X^+ \equiv \max(X, 0)$ . Finally, note that these source terms take slightly different forms in different versions of the multcloud model such as Khouider and Majda (2006b) and Khouider and Majda (2008b).



### 3. Convectively coupled equatorial waves in the multi-cloud model

In this section, we exhibit some typical solutions of the multcloud model equations (1)–(6) in the form of linear waves and long-time non-linear simulations.

For the linear waves, the base state is a state of radiative–convective equilibrium (RCE). RCE is a homogeneous (in space and time) steady state solution for the governing equations (1)–(6) around which waves grow and oscillate. In the multcloud model, an RCE solution is determined by fixing three important climatological parameters, the long-wave radiative cooling rate  $Q_{R,1}^0$ , the discrepancy between the boundary layer equivalent potential temperature and its saturation value,  $\theta_{eb}^* - \bar{\theta}_{eb}$ , and the discrepancy between the boundary layer and midtropospheric equivalent potential temperatures,  $\bar{\theta}_{eb} - \bar{\theta}_{em}$ . They are fixed according to climatological values that are recorded in the tropics Khouider and Majda (2006b, 2008b):  $Q_{R,1}^0 = 1 \text{ K day}^{-1}$ ,  $\theta_{eb}^* - \bar{\theta}_{eb} = 10 \text{ K}$  while  $10 \leq \bar{\theta}_{eb} - \bar{\theta}_{em} \leq 20 \text{ K}$  or higher/lower according to whether we want to study a case of a dry or a moist middle troposphere. More details on the construction of climatologically sound RCE solutions for the multcloud model are found in Khouider and Majda (2006b,a, 2008b).

The PDE system (1)–(6) is then linearized around the relevant RCE solution and linear solutions are sought on the form  $U(x, t) = \hat{U} \exp[i(kx - \omega t)]$ , where  $U$  is the vector of diagnostic variables. Here  $k$  is the zonal wavenumber and  $\omega = \omega(k)$  is the generalized phase determined as an eigenvalue of the corresponding linear system, for a fixed value of  $k$ , while  $\hat{U}(k)$  is the associated eigenvector. The real part of  $\omega(k)$  defines the phase speed of the wave solution:  $c(k) = \Re(\omega(k))/k$  while the imaginary part represents its growth rate.

Before proceeding to the study of linear wave solution to the PDE system, it is important to select RCE's that are stable to small perturbation. This is easily achieved by looking at solutions of the linear system when  $k = 0$ , which essentially represents solutions to the zonally averaged linear solutions. As shown in Khouider and Majda (2006b) and Khouider and Majda (2006a), this system exhibits interesting bifurcation behavior with respect to the model parameters. A typical stability diagram of the background RCE solution with respect to the parameters  $\alpha_c, \alpha_2$  and  $\bar{\theta}_{eb} - \bar{\theta}_{em}$  is shown in Figure 2. Such diagrams are used as guidelines to select the appropriate parameters for the multcloud model (Khouider and Majda 2006b,a, 2008b).

However, the important characteristic of the multcloud model is that, in the appropriate parameter regime, it exhibits a scale selective instability of wave solutions that have several key physical and dynamical features resembling observed convectively coupled equatorial waves. In Figures 3 and 4, we show linear and non-linear solutions for the multcloud equations obtained in the case of a simple flow above the equator, where the beta-effect is ignored. When the full (nonlinear) multcloud equations are integrated numerically, for a long enough time, with an initial condition consisting of the RCE solution plus a small random perturbation, the solution goes to a statistical steady state that exhibits the wave-like disturbances that have the same features as their linear equivalents, including a reduced phase speed of roughly  $17 \text{ m s}^{-1}$  and a front-to-rear vertical tilt in wind, temperature and heating field. In particular, note that the nonlinear simulation is characterized by packets of synoptic scale waves moving at about  $17 \text{ m s}^{-1}$  and have a planetary scale wave envelope moving in the opposite direction at a slower speed of  $5 \text{ to } 6 \text{ m s}^{-1}$ , mimicking observed CCWs evolving within the MJO envelope. Consistent with the “self-similarity” of tropical convection across scales,

the planetary-scale envelope has the same front-to-rear tilted structure as the synoptic scale waves, though only the synoptic scale waves are linearly unstable.

Moreover, when the beta-effect is included the multicloud model exhibits instabilities corresponding to the full spectrum of convectively coupled waves seen in the observational records (Takayabu 1994; Wheeler and Kiladis 1999), with comparable length scales and phase speeds, namely, Kelvin, westward inertio-gravity waves, and  $n = 0$  eastward mixed Rossby-gravity (MRG) or Yanai waves (Khouider and Majda 2008a; Han and Khouider 2010). Similarly, to the rotation-free case, all the simulated CCW solutions exhibit a front-to-rear tilted vertical structure as in nature. While westward MRG waves and Rossby waves are missing in the multicloud model linearized about a homogeneous RCE, they are recovered in the case of a meridional barotropic shear background, mimicking the climatological jet-stream (Han and Khouider 2010). The combination of the results shown in Khouider and Majda (2008a) and Han and Khouider (2010), which are summarized in Figure 5 demonstrate clearly that the multicloud model with rotation reproduces the full spectrum of convectively coupled waves that are reported in the observational literature (Takayabu 1994; Wheeler and Kiladis 1999).

To conclude this section, we note that the results in Figure 3–5 are obtained with the typical synoptic scale convective time scales  $\tau_{conv} = 2$  hours,  $\tau_s = 3$  hours and  $\tau_c = 1$  hours, which are the estimated time scales of the deep convective, stratiform, and congestus clouds. Comparable values are also used in the stochastic multicloud model (Khouider et al. 2010; Frenkel et al. 2012).

## 4. The MJO analog wave

By exploiting a self-similarity argument of tropical convective systems (Majda 2007; Kiladis et al. 2009), the multicloud model can be tuned toward a planetary and intra-seasonal scale instability of a wave that resembles the tropical intra-seasonal oscillation i.e, the MJO, as regards flows along the equator. This is accomplished in Majda et al. (2007) by setting the convective time scales to

$$\tau_{conv} = 12 \text{ hours, and } \tau_c = \tau_s = 7 \text{ days.}$$

Recall that for the case of the synoptic scale waves above, we have  $\tau_{conv} = 2$  hours,  $\tau_c = 1$  hour and  $\tau_s = 3$  hours. The main effect of this change in parameter value is to shift the instability band to larger scales in both time and space. Consistently, numerical simulations with these parameter values yield a solution with the following attractive features that essentially characterize the east-west flow of the MJO above the equator, as shown in Figure 6 (Majda et al. 2007):

- A. An actual propagation speed of roughly  $5 \text{ m s}^{-1}$  as predicted by linear theory.
- B. A wavenumber 2 structure for the low-frequency planetary-scale envelope with distinct active and inactive phases of deep convection.
- C. An intermittent turbulent chaotic multiscale structure within the wave envelope involving embedded westward and eastward-propagating deep convection events.
- D. Qualitative features of the low-frequency averaged planetary-scale envelope from the observational record in terms of, e.g., vertical structure of heating and westerly wind burst.

## 5. GCM simulation of the MJO and convectively coupled waves

Here we show an MJO solution produced by the multcloud model when implemented in the next generation climate model of the National Center for Atmospheric Research (NCAR), namely, the High Order Modeling Environment (HOMME) dynamical core. HOMME is a highly scalable parallel code for the atmospheric general circulation based on the discretization of the primitive equations on the sphere using high order spectral elements in the horizontal and finite differences in the vertical. The interested reader is invited to look into the code development papers Dennis et al. (2005); Taylor et al. (2008) and the online documentation found on the NCAR website. Here the discussion will be limited to a brief description of the strategy adopted to implement the multcloud parameterization in HOMME, which provides the added condensational heating to the otherwise dry model to produce realistic MJO and convectively coupled waves solutions as reported in Khouider et al. (2011).

The first step to incorporate the multcloud model in HOMME consists in designing the proper vertical profiles for the heating field associated with the three cloud types: congestus, deep, and stratiform. We use the vertical normal modes of Kasahara and Puri (1981). The two eigenfunctions,  $\phi_1, \phi_2$ , corresponding to the first and second baroclinic modes, are plotted in Figure 7 (A) together with the associated heating profiles given by the temperature basis functions,  $\psi_j = \frac{1}{p_B - p_T} \int_{p_T}^p \phi_j(p') dp'$   $j=1,2$ , according to the hydrostatic balance equation. The function  $\psi_1$  is used to fix the vertical profile for deep convective heating and  $\psi_2$  is accordingly used for both stratiform and congestus clouds. The heating is set to zero above roughly 200 hPa to avoid spurious heating in the upper atmosphere.

With the heating rates  $H_d, H_s, H_c$  parameterized as in the idealized case presented above and the vertical average moisture equation rederived according to the new basis functions  $\phi_j, \psi_j$  (instead of the cosines and sines), the HOMME full primitive equations are forced by the total heating field  $H(x, y, p) = H_d(x, y)\psi_1(p) + (H_c(x, y) - H_s(x, y))\psi_2(p)$ . The resulting coupled model is solved on an aquaplanet with a uniform surface evaporation and a standard value of radiative cooling: 1 K/day. The moisture and temperature anomalies are initialized to a tropical mean profile which is also used to fix the Brunt-Väisälä frequency profile in the Kasahara and Puri code for the normal modes which is solved once for all at the beginning of the simulation.

In the appropriate parameter regime (Khouider et al. 2011), the coupled HOMME-multicloud model yields a solution consisting of two MJO-like waves that move eastward at roughly  $5 \text{ m s}^{-1}$  somewhat similar to the two TOGA-COARE MJO events reported in Yanai et al. (2000). This is illustrated by (B) the x-t contours of the zonal velocity and deep convection, (C) the zonal structure of the MJO filtered zonal velocity, (D) the filtered vorticity, and (E) the vertical structure of the filtered zonal velocity shown in Figure 7. Note in particular the MJO solution has the same tilted structure, intraseasonal period, and imbedded mesoscale turbulent fluctuations in the deep convective heating as in the case of the MJO analog of Figure 6 and in addition, the vorticity field is characterized by a quadrupole vortex surrounding the westerly-wind burst. The interested reader is referred to the original paper (Khouider et al. 2011) for more discussion of this solution and others. In particular, the whole spectrum of synoptic scale convectively coupled waves is reproduced in the appropriate parameter regime.

## REFERENCES

- Arakawa, A. and W. H. Shubert, 1974: Interaction of a cumulus cloud ensemble with the large-scale environment. part i. *J. Atmos. Sci.*, **31**, 674–701.
- Biello, J. and A. Majda, 2005: A multi-scale model for the madden–julian oscillation. *J. Atmos. Sci.*, **62**, 1694–1721.
- Charney, J. G. and A. Eliassen, 1964: On the growth of the hurricane depression. *J. Atmos. Sci.*, **21**, 68–75.
- Craig, G. C. and S. L. Gray, 1996: CISK or WISHE as the mechanism for tropical cyclone intensification. *J. Atmos. Sci.*, **53**, 3528–3540.
- Dennis, J., A. Fournier, W. Spatz, A. St-Cyr, M. Taylor, S. J. Thomas, and H. Tufo, 2005: High resolution mesh convergence properties and parallel efficiency of a spectral element atmospheric dynamical core. *Int. J. High Perform. Comput. Appl., Special Issue on Climate Modeling. Eds. J.B. Drake, P. Jones, and G. Carr.*, **19**, 225–245.
- Dunkerton, T. J. and F. X. Crum, 1995: Eastward propagating 2- to 15-day equatorial convection and its relation to the tropical intraseasonal oscillation. *J. Geophys. Res.*, **100**, 25 781–25 790.
- Emanuel, K. A., 1987: An air-sea interaction model of intraseasonal oscillations in the tropics. *J. Atmos. Sci.*, **44**, 2324–3240.

- Emanuel, K. A., J. D. Neelin, and C. S. Bretherton, 1994: On large-scale circulations in convecting atmosphere. *Quart. J. Roy. Meteor. Soc.*, **120**, 1111–1143.
- Frenkel, Y., A. J. Majda, and B. Khouider, 2012: Using the stochastic multcloud model to improve tropical convective parameterization: A paradigm example. *J. Atmos. Sci.*, **69**, 1080–1105.
- Frierson, D., A. Majda, and O. Pauluis, 2004: Dynamics of precipitation fronts in the tropical atmosphere. *Comm. Math. Sciences*, **2**, 591–626.
- Fuchs, Z. and D. Raymond, 2002: Large-scale modes of a nonrotating atmosphere with water vapor and cloud-radiation feedbacks. *J. Atmos. Sci.*, **59**, 1669–1679.
- Haertl, P. and G. N. Kiladis, 2004: On the dynamics of two day equatorial disturbances. *J. Atmos. Sci.*, **61**, 2707–2721.
- Han, Y. and B. Khouider, 2010: Convectively coupled waves in a sheared environment. *J. Atmos. Sci.*, **67**, 2913–2942.
- Hayashi, Y., 1971: Large-scale equatorial waves destabilized by convective heating in the presence of surface friction. *J. Meteor. Soc. Japan*, **49**, 458–466.
- Johnson, R. H., T. M. Rickenbach, S. A. Rutledge, P. E. Ciesielski, and W. H. Schubert, 1999: Trimodal characteristics of tropical convection. *Journal of Climate*, **12** (8), 2397–2418.
- Kasahara, A. and K. Puri, 1981: Spectral representation of three-dimensional global data by expansion in normal mode functions. *Mon. Weather Review*, **109**, 37–51.



- Khouider, B., J. Biello, and A. J. Majda, 2010: A stochastic multcloud model for tropical convection. *Comm. Math. Sci.*, **8** (1), 187–216.
- Khouider, B. and A. J. Majda, 2006a: Multicloud convective parametrizations with crude vertical structure. *Theor. Comp. Fluid Dyn.*, **20**, 351–375.
- Khouider, B. and A. J. Majda, 2006b: A simple multicloud parametrization for convectively coupled tropical waves. Part I: Linear analysis. *J. Atmos. Sci.*, **63**, 1308–1323.
- Khouider, B. and A. J. Majda, 2008a: Equatorial convectively coupled waves in a simple multicloud model. *J. Atmos. Sci.*, **65**, 3376–3397.
- Khouider, B. and A. J. Majda, 2008b: Multicloud models for organized tropical convection: Enhanced congestus heating. *J. Atmos. Sci.*, **65**, 897–914.
- Khouider, B., A. St-Cyr, A. J. Majda, and J. Tribbia, 2011: The MJO and convectively coupled waves in a coarse-resolution GCM with a simple multicloud parameterization. *J. Atmos. Sci.*, **68** (2), 240–264.
- Kiladis, G. N., K. H. Straub, and P. T. Haertel, 2005: Zonal and vertical structure of the madden-julian oscillation. *J. Atmos. Sci.*, **62**, 2790–2809.
- Kiladis, G. N., M. C. Wheeler, P. T. Haertel, K. H. Straub, and P. E. Roundy, 2009: Convectively coupled equatorial waves. *Rev. Geophys.*, **47**, RG2003, doi:10.1029/2008RG000266.
- Lin, X. and R. H. Johnson, 1996: Kinematic and thermodynamic characteristics of the flow over the Western Pacific Warm Pool during TOGA COARE. *J. Atmos. Sci.*, **53**, 695–715.
- Lindzen, R. S., 1974: Wave-CISK in the tropics. *J. Atmos. Sci.*, **31**, 156–179.

- Majda, A. and J. Biello, 2004: A multi-scale model for the intraseasonal oscillation. *Proc. Nat. Acad. Sci.*, **101**, 4736–4741.
- Majda, A. J., 2007: New multi-scale models and self-similarity in tropical convection. *J. Atmos. Sci.*, **64**, 1393–1404.
- Majda, A. J. and B. Khouider, 2002: Stochastic and mesoscopic models for tropical convection. *Proc. Nat. Acad. Sci.*, **99**, 1123–1128.
- Majda, A. J., B. Khouider, G. Kiladis, K. H. Straub, and M. G. Shefter, 2004: A model for convectively coupled tropical waves: Nonlinearity, rotation, and comparison with observations. *J. Atmos. Sci.*, **61**, 2188–2205.
- Majda, A. J. and M. Shefter, 2001a: Models for stratiform instability and convectively coupled waves. *J. Atmos. Sci.*, **58**, 1567–1584.
- Majda, A. J. and M. Shefter, 2001b: Waves and instabilities for model tropical convective parametrizations. *J. Atmos. Sci.*, **58**, 896–914.
- Majda, A. J., S. N. Stechmann, and B. Khouider, 2007: Madden-Julian Oscillation analog and intraseasonal variability in a multcloud model above the equator. *Proc. Nat. Acad. Sci.*, **104**, 9919–9924.
- Mapes, B. E., 1993: Gregarious tropical convection. *J. Atmos. Sci.*, **50**, 2026–2037.
- Mapes, B. E., 2000: Convective inhibition, subgridscale triggering energy, and “stratiform instability” in a toy tropical wave model. *J. Atmos. Sci.*, **57**, 1515–1535.

- Matsuno, T., 1966: Quasi-geostrophic motions in the equatorial area. *J. Met. Jap.*, **44**, 25–41.
- Neelin, J. D. and J. Yu, 1994: Modes of tropical variability under convective adjustment and Madden-Julian oscillation. Part I: Analytical theory. *J. Atmos. Sci.*, **51**, 1876–1894.
- Straub, K. and G. Kiladis, 2002: Observations of a convectively-coupled kelvin wave in the eastern pacific itcz. *J. Atmos. Sci.*, **59**, 30–53.
- Straub, K. H. and G. N. Kiladis, 2003: The Observed Structure of Convectively Coupled Kelvin Waves: Comparison with Simple Models of Coupled Wave Instability. *Journal of Atmospheric Sciences*, **60**, 1655–1668, doi:10.1175/1520-0469(2003)060<1655:TOSOCC>2.0.CO;2.
- Takayabu, Y. N., 1994: Large-scale cloud disturbances associated with equatorial waves. Part I: Spectral features of the cloud disturbances. *J. Meteor. Soc. Japan*, **72**, 433–448.
- Taylor, M., J. Edwards, and A. St-Cyr, 2008: Petascale atmospheric models for the community climate system model: New developments and evaluation of scalable dynamical codes. *J. Phys. Conf. Ser.*, **125**, 012 023.
- Wheeler, M. and G. N. Kiladis, 1999: Convectively coupled equatorial waves: Analysis of clouds and temperature in the wavenumber-frequency domain. *J. Atmos. Sci.*, **56** (3), 374–399.
- Wheeler, M., G. N. Kiladis, and P. J. Webster, 2000: Large scale dynamical fields associated with convectively coupled equatorial waves. *J. Atmos. Sci.*, **57**, 613–640.

- Yamasaki, M., 1969: Large-scale disturbances in a conditionally unstable atmosphere in low latitudes. *Pap. Meteor. Geophys.*, **20**, 289–336.
- Yanai, M., B. Chen, and W. Tung, 2000: The Madden-Julian oscillation observed during the TOGA COARE IOP: Global view. *J. Atmos. Sci.*, **57**, 2374–2396.
- Yano, J.-I., J. C. McWilliams, M. Moncrieff, and K. A. Emanuel, 1995: Hierarchical tropical cloud systems in an analog shallow-water model. *J. Atmos. Sci.*, **52**, 1723–1742.
- Yano, J.-I., M. Moncrieff, and J. C. McWilliams, 1998: Linear stability and single column analyses of several cumulus parametrization categories in a shallow-water model. *Quart. J. Roy. Meteor. Soc.*, **124**, 983–1005.
- Zehnder, J. A., 2001: A comparison of convergence- and surface-flux-based convective parametrizations with applications to tropical cyclogenesis. *J. Atmos. Sci.*, **58**, 283–301.

## List of Figures

- 1 Left: Schematic of the three tropical cloud types interacting with the well-mixed planetary boundary layer above the sea surface through convective updrafts and downdrafts: the trade wind inversion, the freezing level with temperature  $0^{\circ}\text{C}$ , and tropopause layers are shown. Right: Vertical profiles of heating and cooling fields associated with the three cloud types. Figure 1 from Khouider and Majda (2008b). ©2008 American Meteorological Society. Reprinted with permission. 23
- 2 Bifurcation diagram for the homogeneous state RCE (a) in the  $\gamma_2$ - $\alpha_c$  plane for fixed  $\bar{\theta}_{eb} - \bar{\theta}_{em} = 14$  K and (b) in the  $\gamma_2$ - $\bar{\theta}_{eb} - \bar{\theta}_{em}$  plane for fixed  $\alpha_c = .5$ . The regions of positive maximum growth among the  $k = 0$  modes are shaded and a few contours are plotted. Figure 2 from Khouider and Majda (2006b). ©2006 American Meteorological Society. Reprinted with permission. 24
- 3 Top: Scale selective instability in the multcloud model with enhanced congestus closure. Bottom: (x-t) contours of the first baroclinic zonal velocity and moisture anomaly showing streaks corresponding to synoptic scale moist gravity waves moving to the right at  $17 \text{ m s}^{-1}$  and their planetary scale wave-envelopes moving in the opposite direction at  $6 \text{ m s}^{-1}$ . Figures 2 and 5 from Khouider and Majda (2008b). ©2008 American Meteorological Society. Reprinted with permission. 25

- 4 Filtered structure of the synoptic scale moist gravity wave (bottom) and its low-frequency planetary scale envelope (top). The left panel show potential temperature contours while the heating anomalies are contoured on the right panels with the corresponding  $u - w$  velocity arrows are overlaid on top. The + signs on the temperature panels refer to positive anomalies. Figure 7 from Khouider and Majda (2008b). ©2008 American Meteorological Society. Reprinted with permission. 26
- 5 Dispersion diagrams for the multicloud model with rotation. Top: with a homogeneous background. Bottom: with a barotropic-meridional shear zonal wind mimicking the jet stream. Respectively, figure 2 from Khouider and Majda (2008a) and Figure 8 Han and Khouider (2010). ©2008, 2010 American Meteorological Society. Reprinted with permission. 27
- 6 MJO analog wave obtained by convective time scaling for the multicloud model. Left: x-t contours of precipitation showing slowing moving wave envelopes of mesoscale chaotic convective events that evolve within the active phase and propagate in the opposite direction. Right: vertical structure of (a) the total heating, with the  $uw$  velocity overlaid, and (b) the zonal velocity for the moving average of the planetary scale envelope. Figures 2 and 4 from Majda et al. (2007). ©2007 National Academy of Sciences, U.S.A. 28

7 Eigenmode and heating profiles used to implement the multcloud model in HOMME: (A) and the resulting MJO solution: (B) the x-t contours of the zonal velocity and deep convection, (C) the zonal structure of the MJO filtered zonal velocity and (D) filtered vorticity, and (E) vertical structure of the filtered zonal velocity. Figures 1,3,6,8 from Khouider et al. (2011). ©2010 American Meteorological Society. Reprinted with permission.

29

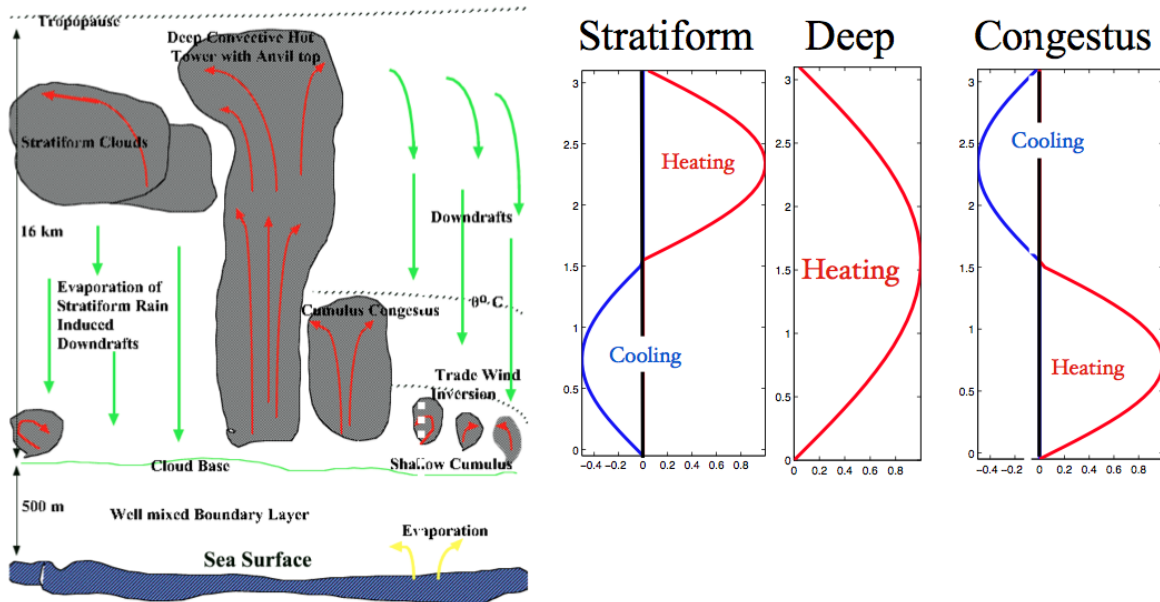


FIG. 1. Left: Schematic of the three tropical cloud types interacting with the well-mixed planetary boundary layer above the sea surface through convective updrafts and downdrafts: the trade wind inversion, the freezing level with temperature  $0^{\circ}\text{C}$ , and tropopause layers are shown. Right: Vertical profiles of heating and cooling fields associated with the three cloud types. Figure 1 from Khouider and Majda (2008b). ©2008 American Meteorological Society. Reprinted with permission.



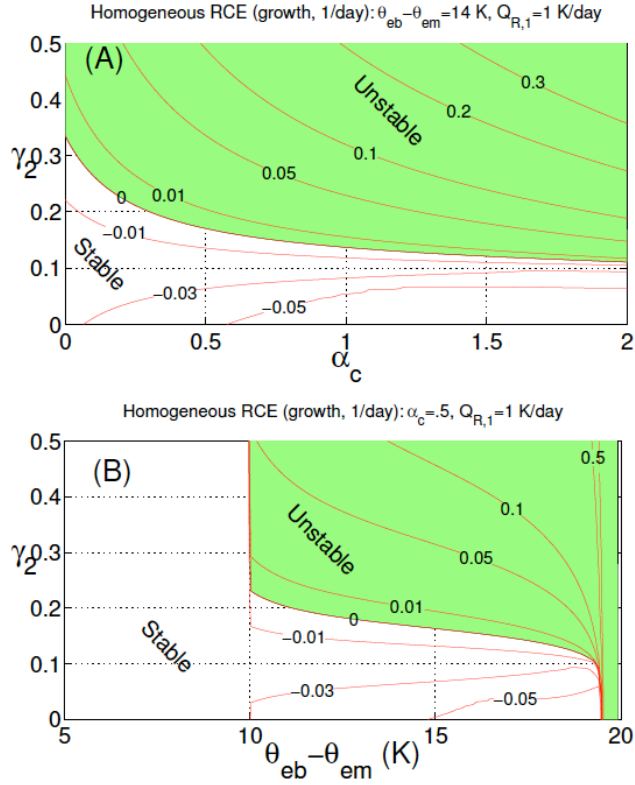


FIG. 2. Bifurcation diagram for the homogeneous state RCE (a) in the  $\gamma_2$ - $\alpha_c$  plane for fixed  $\bar{\theta}_{eb} - \bar{\theta}_{em} = 14$  K and (b) in the  $\gamma_2$ - $\bar{\theta}_{eb} - \bar{\theta}_{em}$  plane for fixed  $\alpha_c = .5$ . The regions of positive maximum growth among the  $k = 0$  modes are shaded and a few contours are plotted. Figure 2 from Khouider and Majda (2006b). ©2006 American Meteorological Society. Reprinted with permission.

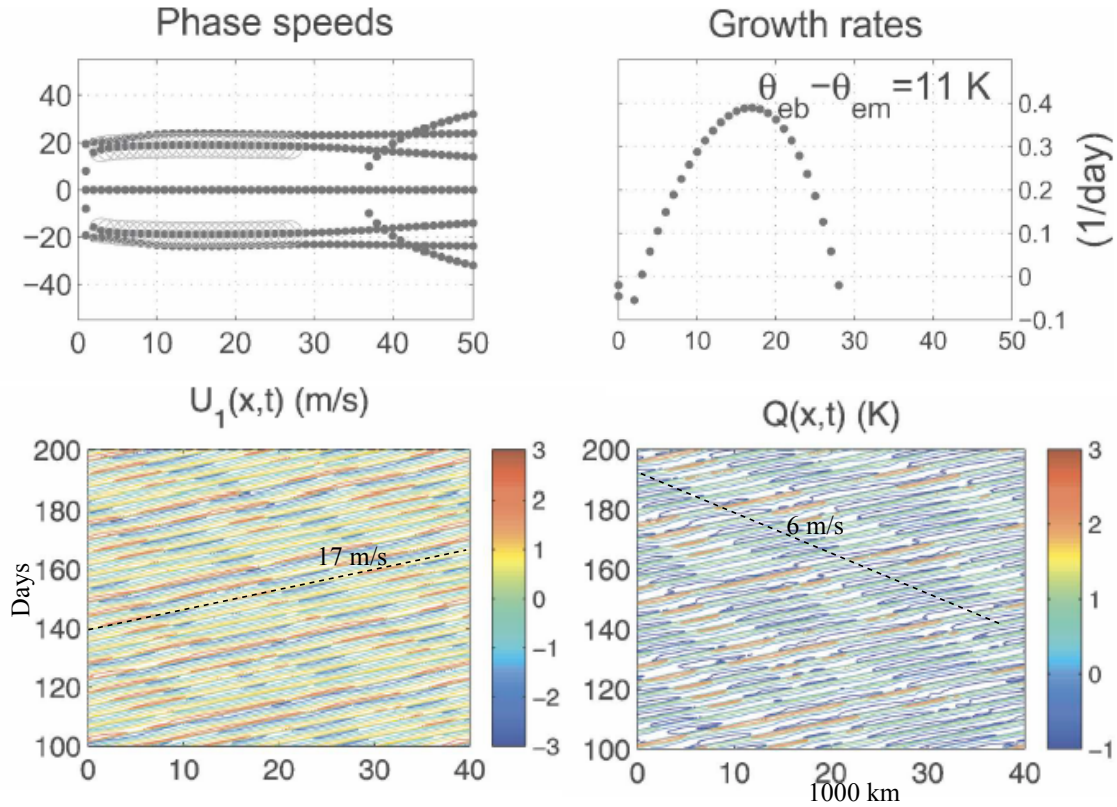


FIG. 3. Top: Scale selective instability in the multicloud model with enhanced congestus closure. Bottom: (x-t) contours of the first baroclinic zonal velocity and moisture anomaly showing streaks corresponding to synoptic scale moist gravity waves moving to the right at  $17 \text{ m s}^{-1}$  and their planetary scale wave-envelopes moving in the opposite direction at  $6 \text{ m s}^{-1}$ . Figures 2 and 5 from Khouider and Majda (2008b). ©2008 American Meteorological Society. Reprinted with permission.

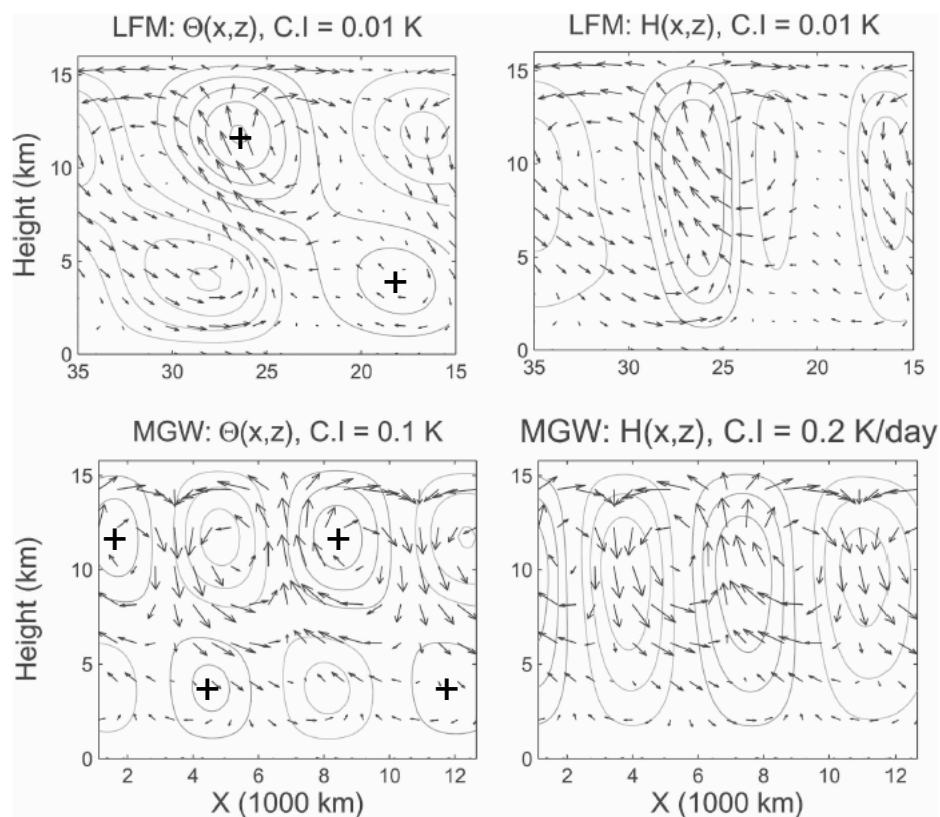


FIG. 4. Filtered structure of the synoptic scale moist gravity wave (bottom) and its low-frequency planetary scale envelope (top). The left panel show potential temperature contours while the heating anomalies are contoured on the right panels with the corresponding  $u - w$  velocity arrows are overlaid on top. The + signs on the temperature panels refer to positive anomalies. Figure 7 from Khouider and Majda (2008b). ©2008 American Meteorological Society. Reprinted with permission.

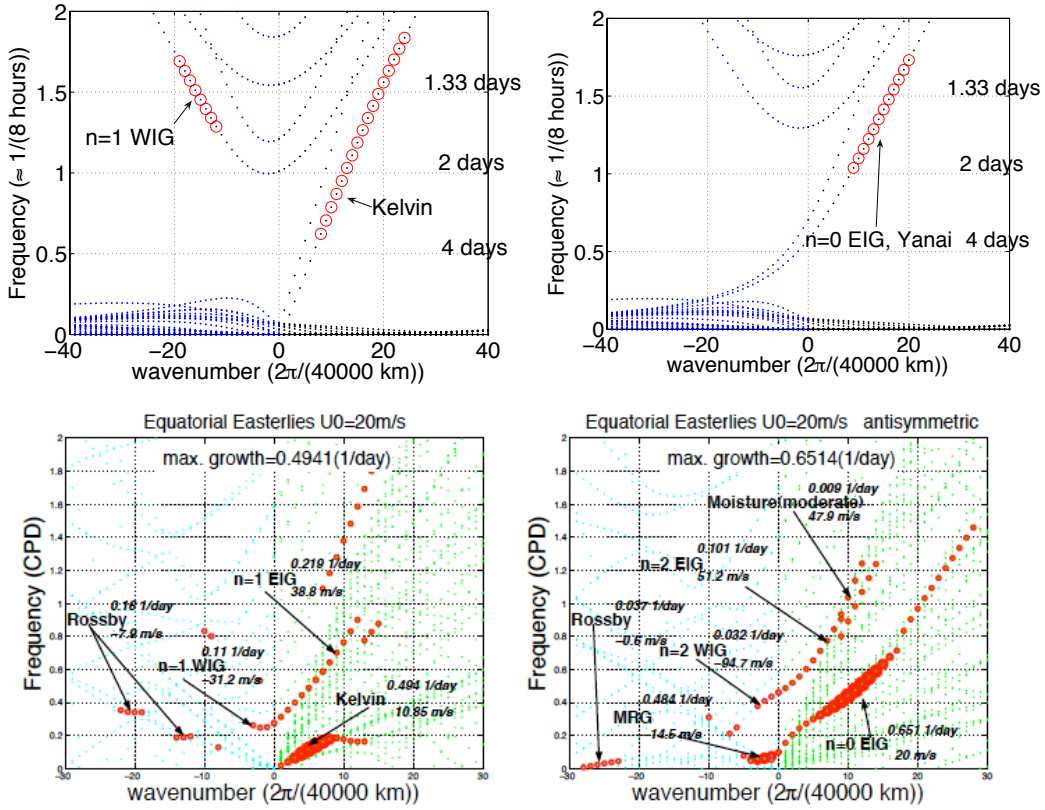


FIG. 5. Dispersion diagrams for the multcloud model with rotation. Top: with a homogeneous background. Bottom: with a barotropic-meridional shear zonal wind mimicking the jet stream. Respectively, figure 2 from Khouider and Majda (2008a) and Figure 8 Han and Khouider (2010). ©2008, 2010 American Meteorological Society. Reprinted with permission.

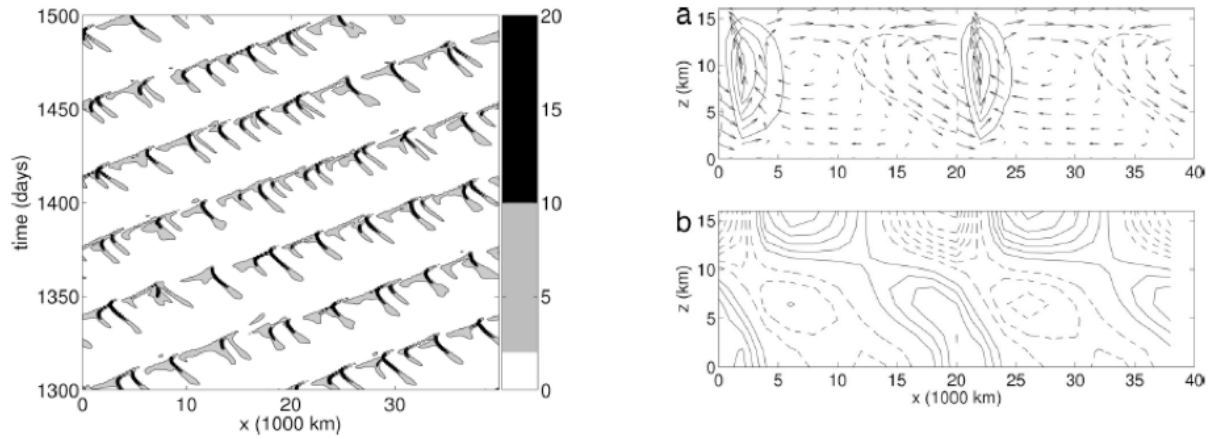


FIG. 6. MJO analog wave obtained by convective time scaling for the multicloud model. Left:  $x$ - $t$  contours of precipitation showing slowing moving wave envelopes of mesoscale chaotic convective events that evolve within the active phase and propagate in the opposite direction. Right: vertical structure of (a) the total heating, with the  $uw$  velocity overlaid, and (b) the zonal velocity for the moving average of the planetary scale envelope. Figures 2 and 4 from Majda et al. (2007). ©2007 National Academy of Sciences, U.S.A.

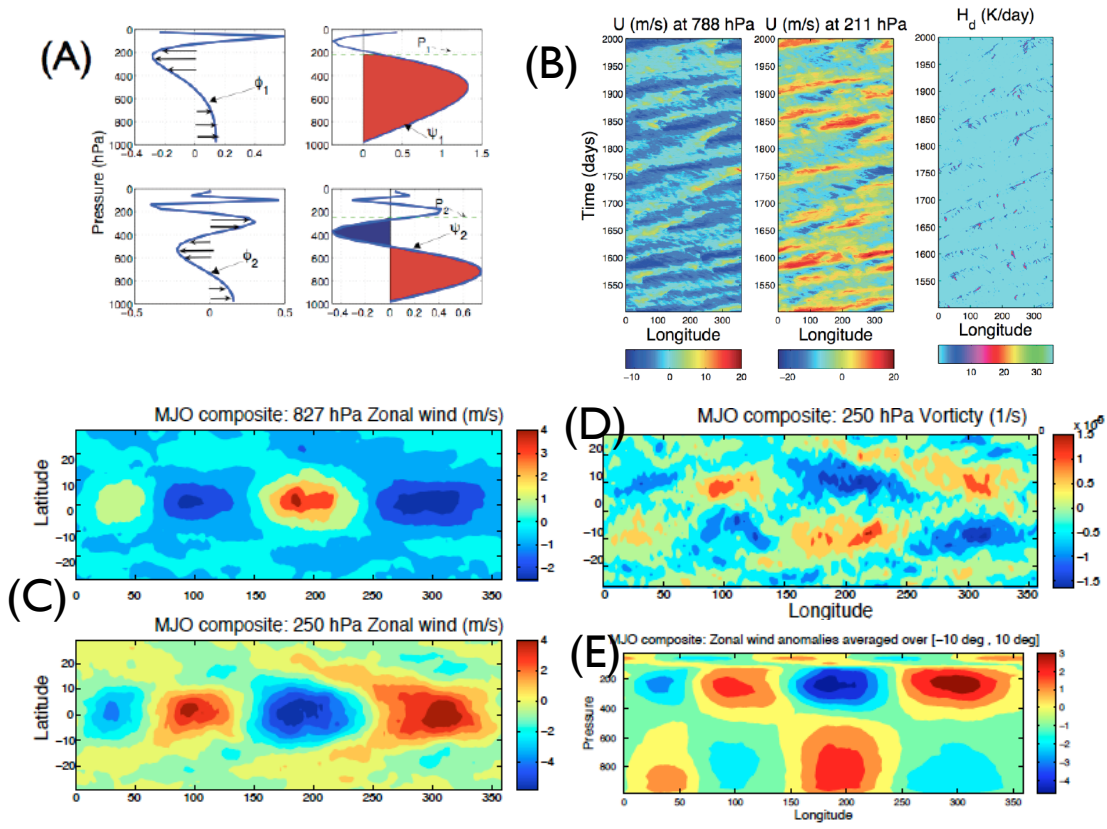


FIG. 7. Eigenmode and heating profiles used to implement the multicloud model in HOMME: (A) and the resulting MJO solution: (B) the x-t contours of the zonal velocity and deep convection, (C) the zonal structure of the MJO filtered zonal velocity and (D) filtered vorticity, and (E) vertical structure of the filtered zonal velocity. Figures 1,3,6,8 from Khouider et al. (2011). ©2010 American Meteorological Society. Reprinted with permission.